



OPEN Nano-liposomal delivery of *Gracilaria corticata* bioactive peptides for improved stability and controlled gastrointestinal release

Mojtaba Heydari-Majd¹, Farideh Mahmoodi², Hassan Rezaeinia³, Ramin Saravani^{4,5}✉, Mohammad Molaveisi⁶✉, Mostafa Shahidi Noghbi⁶, Heidar Meftahizade⁷ & Somayeh Dahmardeh^{8,9}

This study aimed to develop and evaluate a liposomal nano-delivery system for bioactive peptide fractions (PFs) derived from *Gracilaria corticata* algae proteins. The peptides were obtained by enzymatic hydrolysis using alcalase, pancreatin, and trypsin. The resulting PF-loaded nanoliposomes were characterized in terms of degree of hydrolysis (DH), particle size, ζ -potential, encapsulation efficiency (EE), and antioxidant capacity (DPPH and ABTS assays). Among the tested enzymes, alcalase produced hydrolysates with the highest DH (33%) and EE (84%). The particle size of nanoliposomes ranged from 68.1 to 78.1 nm, with PDI values between 0.28 and 0.32, indicating good size uniformity. ζ -potential values became more negative upon PF encapsulation (from -7.90 to -15.80 mV), enhancing colloidal stability. Antioxidant activity of the PF-loaded liposomes was preserved, with maximum DPPH and ABTS radical scavenging observed for alcalase and pancreatin hydrolysates, respectively. Hydrolysates obtained with alcalase were chosen for further studies. Further structural and thermal analyses (TEM, FTIR, and DSC) confirmed successful PF encapsulation and improved thermal stability. TEM and FTIR analyses confirmed the spherical morphology and successful peptide encapsulation within the liposomal bilayer. In vitro release studies in simulated gastric and intestinal fluids demonstrated sustained release, with minimal PF release (7.45%) in gastric conditions and controlled release up to 95.4% under intestinal conditions. These findings suggest that nano-liposomal encapsulation is an effective strategy to enhance the stability, bioactivity, and delivery of marine-derived peptides in functional food or nutraceutical applications.

Keywords Nano-liposomes, Bioactive peptides, *Gracilaria corticata*, Enzymatic hydrolysis, Sustained release

Nowadays, there is an escalating attention towards the development of functional foods, which are intentionally formulated to boost human health and overall well-being. Thus, researchers are exploring novel sources of bioactive compounds that can serve as health-promoting agents in practical food applications^{1–3}. Marine organisms, which account for approximately half of the world's biodiversity, are a rich source of diverse beneficial compounds. In the realm of marine organisms, seaweeds are classified as macroalgae, and are further subdivided into three main categories: *Phaeophyta* (brown algae), *Rhodophyta* (red algae), and *Chlorophyta* (green algae)⁴.

Gracilaria corticata, a red macroalga, is widely distributed in tropical and subtropical coastal regions. Seaweeds such as *G. corticata* can concentrate minerals from seawater, reaching mineral content 10–20 times

¹Department of Agriculture and Natural Resources, Ardakan University, P.O. Box 184, Ardakan, Iran. ²Department of Food Science and Technology, Quchan Branch, Islamic Azad University, Quchan, Iran. ³Department of Food Nanotechnology, Research Institute of Food Science and Technology (RIFST), Km 12 Mashhad-Quchan Highway, P.O. Box 91895/157/356, Mashhad, Iran. ⁴Cellular and Molecular Research Center, Research Institute of Cellular and Molecular Sciences in Infectious Diseases, Zahedan University of Medical Sciences, Zahedan, Iran. ⁵Department of Clinical Biochemistry, School of Medicine, Zahedan University of Medical Sciences, Zahedan, Iran. ⁶Department of Food Chemistry, Research Institute of Food Science and Technology, Mashhad-Quchan Highway, PO Box 91735-147, Mashhad, Iran. ⁷Department of Horticultural Sciences, Faculty of Agriculture and Natural Resources, Ardakan University, Ardakan, Iran. ⁸Faculty of Pharmacy, Zabol University of Medical Sciences, Zabol, Iran. ⁹Zahedan University of Medical Sciences, Zahedan, Iran. ✉email: raminsaravani@gmail.com; molaveisi@sdu.edu.cn

higher than terrestrial plants, making them valuable for human nutrition. Chlorophyll, an important pigment in algae, demonstrates positive effects on inflammation, oxidation, and wound healing by acting as a free radical scavenger and protecting lymphocytes against oxidative DNA damage. Moreover, various bioactive compounds including phenols, polyphenols, terpenes, steroids, halogenated ketones, alkanes, fucoxanthin, polyphloroglucinol, and bromophenols have been isolated from these organisms^{5,6}. Specifically, *G. corticata* exhibits substantial protein content (up to 40% dry weight) with a balanced amino acid profile rich in aspartic acid, glutamic acid, alanine, and glycine, making it an ideal precursor for bioactive peptide production⁶. This species has been traditionally used in food and phycocolloid industries, and recent studies have highlighted its antioxidant, antimicrobial, and anti-inflammatory properties, largely attributed to its protein-derived peptides⁶. Therefore, extracting proteins from seaweeds, particularly *Gracilaria* species, is crucial for the food industry due to their significant value as biological compositions.

The use of proteins is limited due to their sensitivity, instability, solubility, digestive limitations, allergenic compounds, and loss of functionality when reacting with other compounds⁷. A key approach to addressing these challenges is to alter the protein structure and generate peptide fractions (PFs) through enzymatic hydrolysis. Some key benefits of PFs over antioxidants and synthetic compounds include low cost, easy absorption, safety, and high nutritional value. PFs also have high digestibility, low allergenicity, and stability in various conditions and formulas, while maintaining their activity and biological performance⁸. Various studies have been conducted on the enzymatic hydrolysis of a range of proteins, including mung bean⁹, Brazilian soy protein¹⁰, bighead carp¹¹, colostrum whey¹², and maize¹³, to obtain bioactive peptides with antioxidant or antimicrobial activities. While these investigations confirm the potential of enzymatic treatment to generate functional peptides, most have focused on terrestrial sources or well-studied marine organisms, with limited exploration of red algae such as *G. corticata*. Moreover, few of these studies evaluated the structural stability, encapsulation behavior, or gastrointestinal fate of the resulting peptides factors crucial for real-world application in food or nutraceutical products. However, despite their promising biological activities, PFs still face several challenges related to storage stability, biostability and practical application when incorporated into food products, pharmaceuticals and dietary supplement⁷.

Researchers aim to develop micro/nano encapsulation techniques to protect bioactive compounds from harsh environmental conditions and ensure precise release, despite the drawbacks mentioned¹⁴. Several methods can be used to encapsulate bioactive compounds, such as spray drying, nano-liposome and nano-phytosome carrier, electrospinning, co-precipitation, freeze drying, and emulsification^{15–18}. Among them, nanoliposomes are self-assembled structures resulting from the association of lipid molecules in aqueous solution¹⁹. Several studies have utilized nano-liposomes to encapsulate PFs derived from various sources, including *Spirulina platensis*²⁰, walnut²¹, soy protein²², and fish²³, demonstrating the effectiveness of liposomal systems for improving peptide stability and functionality.

Despite extensive reports on nano-liposomal encapsulation of protein and peptide hydrolysates from various marine and plant sources, a major gap remains regarding the delivery of *highly labile marine-derived peptides* that are particularly susceptible to thermal processing and gastrointestinal degradation. Red algae-derived peptides, including those from *Gracilaria corticata*, often exhibit promising bioactivities but suffer from limited stability, which restricts their translation into functional food and nutraceutical applications.

In this context, the novelty of the present study does not lie merely in the selection of *G. corticata* as a peptide source, but rather in addressing these intrinsic stability limitations through a systematically evaluated nano-liposomal delivery system. By combining enzymatic hydrolysis with liposomal encapsulation, this work provides an integrated assessment of physicochemical properties, structural interactions, thermal behavior, antioxidant activity preservation, and pH-responsive gastrointestinal release. The results demonstrate that liposomal encapsulation can effectively protect sensitive marine peptides under gastric conditions while enabling controlled and near-complete release in intestinal environments, thereby offering a practical and application-oriented strategy for utilizing unstable yet bioactive marine peptides in functional food and nutraceutical formulations.

This study aims to address this gap by developing a liposomal nano-delivery system for *G. corticata*-derived peptides, systematically characterizing their physicochemical properties, antioxidant capacity, and in vitro release behavior in digestive environments. The findings offer novel insights into the potential of red algae-based peptides for applications in functional food and nutraceutical formulations.

Materials and methods

Chemicals and samples

Algae powder derived from *G. corticata* was purchased from Algae Bio-resources Development Company (Shiraz, Iran). For enzymolysis process, alcalase (*Bacillus licheniformis*, ≥ 2.4 AU/g), pancreatin (porcine pancreas, P1750, 4 × USP specifications) and trypsin (bovine pancreas, activity 2–4 U/mg) were obtained from Sigma-Aldrich (St. Louis, Missouri, USA) and then, stored in the refrigerator. Soy lecithin (lipoid, Germany), trichloroacetic acid (TCA), bovine serum albumin (BSA) and glycerol were purchased from Merck Company (Weiterstadt, Germany). To evaluate the antioxidant activity, DPPH (1,1-Diphenyl-2-picrylhydrazyl) and ABTS (2,20 -azino-bis (3-ethylbenzothiazoline-6-sulfonic acid) diammonium salt), were purchased from Gibco Chemical Co., (Grand Island, NY, USA). The bicinchoninic acid (BCA) kits protein assay was acquired from Thermo Fisher Scientific (Waltham, MA). Pepsin and pancreatin used for preparation of simulated gastric and intestinal fluids were purchased from Sigma-Aldrich (St. Louis, MO, USA). Potassium chloride (KCl) and potassium dihydrogen phosphate (KH_2PO_4) were obtained from Merck (Darmstadt, Germany). Only high-quality chemicals and reagents were used in the study without any additional purification.

Proximate composition of *Gracilaria corticata* algae powder

The approximate composition of *G. corticata* algae powder (moisture, ash, fat and crude protein) was determined according to the AOAC method²⁴. Moisture content was measured by drying 5 g of sample in a hot air oven (Memmert, Germany) at 105 °C until constant weight. Ash content was determined by incinerating 3 g of dried sample in a muffle furnace (Nabertherm, Germany) at 550 °C for 6 h. Crude protein content was estimated using the Kjeldahl method, with a nitrogen-to-protein conversion factor of 6.25. Crude fat content was extracted using Soxhlet extraction with petroleum ether. The total carbohydrate content of *G. corticata* was determined by the phenol–sulfuric acid method⁶.

Extraction of *Gracilaria corticata* algae protein

The protein concentrate from *G. corticata* algae powder was produced using a modified method suggested by Mohammadi et al.⁷ in five steps. The first stage involves removing fat from *G. corticata* algae powder using hexane solvent (1:4 w/v). The second and third stages include extracting and precipitating proteins in a saline solution with pH 9.25, and adjusting the pH to the isoelectric point of 4.2 using 0.5 M HCl, respectively. The fourth step is neutralizing the protein with 1 M NaOH and adjusting the pH to 7.2. The final step is freeze-drying (Telstar, Terrassa, Spain) the precipitates. Following the extraction steps, the protein yield was calculated as (Eq. 1):

$$\text{Protein yield (\%)} = \frac{\text{Mass of extracted protein (g)}}{\text{Mass of initial alga powder (g)}} \times 100. \quad (1)$$

The mean protein yield was found to be 84 ± 1.2% (w/w, dry basis), demonstrating effective protein recovery suitable for downstream hydrolysis.

Enzymatic hydrolysis

The protein was mixed with water at a 3% concentration for the hydrolysis process. The enzymes trypsin (pH 8, temperature 37 °C), pancreatin (pH 8, temperature 37 °C), and alcalase (pH 8, temperature 50 °C) were used in the hydrolysis process in 6% (W/W, enzyme to the substrate) for 240 min. At the end of hydrolysis, the enzyme activity was terminated by heating the mixture at 90 °C for 10 min. The resulting dispersion was cooled to ambient temperature and centrifuged at 5000 × g* for 10 min (Hettich Zentrifugen, Germany). The supernatants containing the soluble peptide fractions (PFs) were collected and lyophilized using a freeze-dryer (Telstar, Terrassa, Spain) then stored at –20 °C until further use²⁰.

Evaluation of degree of hydrolysis (DH)

To achieve this goal, equal volumes of PFs and TCA (0.44 M) were mixed and subsequently stored at refrigeration (4 °C) for 10 min. In the following, the aforementioned mixture was centrifuged (Sigma, 3–30 K; Germany; 10,000 rpm for 10 min) and the obtained soluble protein was calculated using the Bradford²⁵ method, as well as, the standard solution of BSA. Finally, the value of DH was calculated based on Eq. (2):

$$\text{DH (\%)} = \frac{\text{Protein (TCA + supernatant)}}{\text{Protein (PFs suspension)}} \times 100. \quad (2)$$

Preparation of PFs-loaded nano-liposomes

Liposomes were prepared using the thin-film hydration method. A mixture of 120 mg soybean lecithin and 30 mg cholesterol was dissolved in ethanol¹. The organic solvent was then removed under vacuum with a rotary evaporator to form a lipid film, maintained at 40 °C for 15 min. The dried lipid film was hydrated with 0.01 M phosphate-buffered saline (PBS), pH 7.0, in a water bath at 37 °C for 60 min. To make peptide-loaded liposomes, the lipid film was rehydrated with 15 mL of PBS (0.01 M, pH 7.0) containing PFs. The resulting liposomal suspension was subjected to probe-type sonication at 360 W for 5 min. The ultrasonication process was carried out at a 20 kHz frequency in an ice bath with on/off pulse mode, maintaining temperatures between 25 and 40 °C to produce single-layer nanoliposomes. The process involved two phases: (1) a 30-s sonication phase in pulsed cycle mode set to two, and (2) a 1-min non-sonication (standing) phase. These phases were alternated, with the sonication phase repeated four times and the non-sonication phase repeated three times. The liposomes were stored at 4 °C before use.

Measurement of particle size, ζ-potential and encapsulation efficiency (EE) of nano-liposomes

Particle size and ζ-potential of each sample were measured before and after PFs loading using a Zetasizer Nano ZS (Malvern Instruments Ltd., Malvern, UK) at 25 °C, with 3 replications²⁶.

The EE of the PFs in nano-liposomes was determined using an Amicon Ultra-15 centrifugal filter unit equipped with a 10 kDa molecular weight cut-off (MWCO) membrane (PLGC Ultracel-PL, Cork, Ireland). This membrane size was selected to ensure complete retention of the peptide-loaded liposomes (size range 68–78 nm) while allowing unencapsulated (free) peptides to pass through. After filtration, centrifugation was performed at 3000 × g* for 10 min, and the amount of free peptides in the filtrate was quantified using the Bradford method²⁵:

$$\text{EE (\%)} = \frac{\text{Total PF content} - \text{Amount of free PF}}{\text{Total PF content}} \times 100. \quad (3)$$

Antioxidant capacity

To determine the antioxidant capacity of the encapsulated peptides, the PFs-loaded nanoliposomes were first subjected to heat treatment at 100 °C for 5 min in a water bath to ensure complete release of the peptides from the lipid vesicles. Free peptide fractions (unencapsulated) were analyzed without heat treatment. After heating, the released peptide content was assessed using the DPPH radical scavenging assay²⁷ and the ABTS radical scavenging assay⁷. All measurements were performed in triplicate.

Structural, thermal and morphological properties of PFs-loaded nano-liposomes

FTIR spectroscopy

Fourier transform infrared spectroscopy (FT-IR) were recorded using a Thermo Nicolet Avatar 370 spectrometer (Thermo Fisher Scientific, USA) to identify the functional groups, interactions formed between the nano-carrier and the PFs, and the structural changes of the microstructures. The samples were formed into KBr pellets and scanned in the range from 4000 to 400 cm^{-1} with a minimum of 64 scans²⁸.

Thermal analysis

The thermal profile of the new liposome was analyzed using a DSC Maia F3 200 instrument (Netzsch, Germany) under nitrogen flow of 150 mL/min with a heating rate of 10 °C/min from 20 to 300 °C (Heydari-Majd et al. 2020).

Morphology of nano-liposomes

The morphological architecture of peptide fraction-loaded nanovesicles was examined with a transmission electron microscope (TEM, HRTEM, Philips, USA) under conditions of negative staining based on the procedure of Ramezanzade et al.²³. In brief, nanoliposomal samples were diluted 1:30 with deionized water in an attempt to decrease the concentration of the nanovesicles. An equivalent volume of the diluted sample and a solution of 2% ammonium molybdate were mixed for negative staining. After 3 min of incubation at room temperature, the mixture was placed on a carbon-coated copper grid for 5 min. The morphology of the encapsulated peptide was then visualized and imaged at 200 kV accelerating voltage by TEM.

Investigating PFs release in simulated stomach and intestine media

The release rate of PFs were studied in two media that mimic the simulated gastric fluid (SGF) and simulated intestinal fluid (SIF) to evaluate the stability and protective effects of the nanoliposomes coating²⁹. To prepare the SGF, 100 mg of pepsin was dissolved in 5 mL of distilled water containing 0.35 mL of concentrated HCl. Then 100 mg of NaCl was added to the solution. The solution was diluted with distilled water to a final volume of 50 mL. The final pH of the solution was adjusted to 1.2 using concentrated HCl. To make the SIF, 340 mg of potassium phosphate monobasic was dissolved in 10 mL of distilled water. Then 4 mL of 0.2 M NaOH solution and 500 mg of pancreatin were added to the prepared solution. The final volume of the solution was 50 mL and the final pH was 6.8. Samples (1 mL) were incubated in SGF/SIF at 37 °C using a thermomixer (Model RO 300.16, Gerhardt, Germany) at 100 rpm for 2 h (SGF) and 4 h (SIF), respectively. Peptide levels were measured in both media at the desired time intervals based on the peptide measurement method with the BCA kit.

Statistical analysis

All data were statistically analysed by SPSS v21.0 (IBM SPSS, New York, USA) and one-way analysis of variance (ANOVA) followed by Duncan's multiple-range tests. The data's normality was evaluated using the Shapiro–Wilk test, and homogeneity of variances was verified through Bartlett's test. If both assumptions were satisfied, parametric tests like one-way ANOVA were conducted. Differences between averages were considered statistically significant when $p \leq 0.05$.

Results and discussion

Relative composition of alga powder

The biochemical constituents of alga powder, specifically moisture, protein, ash, and fat content, were assessed based on a dry weight basis. The alga powder exhibited average concentrations of 8.33 g, 8.55, 8.72 g, 39.22 g, 45.2 gr and 6.90 g per 100 g of dry weight seaweed for ash, carbohydrate, moisture, protein, polysaccharide and fat, respectively. In a similar study, Rosemary et al.⁶ reported that ash, moisture, protein, and fat contents of *G. corticata* algae powder were 8.10, 8.40, 22.84, and 7.07 (g/100 g dry weight seaweed), respectively. Our study found that algae powder is high in protein and low in fat. Lipids function as an essential storage component for living organisms, supplying sufficient energy during the oxidation process. In general, marine algae are not seen as a prominent source of crude lipids. Protein is important for supplementing the human diet. Red seaweeds such as *G. Corticata* may be a valuable source of food protein and amino acids. Adding high-protein *corticata* seaweed to functional foods may be a beneficial use of this resource.

Physicochemical results of PFs-loaded nano-liposomes

Degree of hydrolysis, mean particle size and polydispersity index (PDI)

The hydrolysis degree (DH) is a key functional trait of PFs. Several factors impact the DH, such as the size and amino acid composition of PFs, biological activity, and the taste of the PFs⁷. Increasing the degree of hydrolysis results in the creation of bitter-tasting peptides in the sample, as well as a shorter chain length and reduced molecular weight distribution. This is caused by more chain breakage, an increase in amino acids, and smaller peptides. The value of DH ranged from 19 to 33% depending on the enzyme type, as shown in Table 1. Enzymatic hydrolysis using alcalase yielded the highest DH (33%) and encapsulation efficiency (84%), while trypsin resulted in the lowest value (19%). This finding is in agreement with the results of Mao et al.³⁰ who investigated the effect

Enzyme type	Degree of hydrolysis (%)	Z-average (nm)	PDI	ζ (mV)		EE (%)
				Free peptide	Encapsulated peptide	
Control	–	57 ± 2.55 ^d	0.18 ± 0.02 ^b	–	– 7.90 ± 0.09 ^d	–
Alcalase	33 ± 1.00 ^a	73 ± 1.50 ^b	0.30 ± 0.02 ^a	– 25.75 ± 0.01 ^b	– 9.53 ± 0.08 ^c	84.10 ± 2.55 ^a
Pancreatin	27 ± 0.93 ^b	78 ± 1.20 ^a	0.32 ± 0.01 ^a	– 27.90 ± 0.02 ^a	– 12.90 ± 0.11 ^b	83.25 ± 2.11 ^a
Trypsin	19 ± 1.25 ^c	68 ± 1.10 ^c	0.28 ± 0.09 ^a	– 25.11 ± 0.01 ^b	– 15.80 ± 0.09 ^a	80.90 ± 2.90 ^a

Table 1. Effect of various hydrolysate enzymes on the physical properties of nano-encapsulated PFs. Different letters in each column (a, b, c) represents a significant difference between treatments ($p < 0.05$). Data are presented as mean ± SD ($n = 3$).

of different proteases (trypsin, pepsin, alcalase and papain) on the degree of casein hydrolysis in cow's milk. In another study, Daud et al.³¹, stated that, alcalase has a high ability in hydrolysis Red Tilapia meat PFs compared to other enzymes. The researchers noted that alcalase operates with a more random and extensive cutting site specificity, unlike other enzymes that tend to have more defined and specific sites.

Particle size in a colloidal nano-carrier system affects indicators like stability, solubility, release of bioactive agents, bioavailability, and gravitational separation. The PDI measures how evenly vesicles are distributed, with values ranging from 0 to 1 in different systems. A high value of this index shows a wide range of particle sizes, suggesting the presence of coarse and uneven particles in the system³². The average particle sizes ranged from 68.1 to 78.1 nm, with acceptable PDI values (0.28–0.32), indicating good uniformity. This was higher than the control capsule, which had a particle size of 57 ± 2.55 nm and a PDI of 0.18. This shows that the liposomes had a suitable particle size and even distribution. The size and PDI of nano-carriers increased after being encapsulated with trypsin hydrolysates, from 57.2 to 68.1 nm and from 0.18 to 0.28, respectively (Table 1). The liposomes grew larger due to the creation of multiple layers of phospholipids made possible by inserting PF. A low PDI suggests a uniform particle size distribution. In simple terms, a low index value means the particles in the distribution system are similar in size and evenly distributed. Similar result has reported an increase in the nano-liposomal size after loading PFs from whitemouth croaker (da Rosa³³). The particle size of nano-liposomes in the present study is suitable for food and pharmaceutical industries.

ζ -potential and EE

Z-potential is the best indicator to determine the surface electrical state of colloidal systems^{34,35}. This parameter indicates the buildup of charge on the immobile layer, the adsorption of opposite ions to the particle surface, and ultimately the level of electrostatic stability²⁶. Lowering the ζ -potential difference below a certain point causes the charged double layer around the particles to collapse, leading to particle aggregation. High ζ -potentials (positive or negative) indicate strong electrostatic repulsion between particles, reducing the frequency of collisions and increasing the physical stability of the liposome suspension⁷. The initial measurement of the ζ -potential for each pure PF indicated values ranging from – 25.11 to – 27.90 mV (Table 1). The pure PF likely has a negative ζ -potential due to its high concentration of glutamic and aspartic amino acids⁶. ζ -potential became more negative after PF loading (– 7.9 to – 15.8 mV), enhancing colloidal stability. This trend may have been caused by the placement of negatively charged PFs on the surfaces of vesicles. The negative charge on the surfaces of the empty nanoliposomes comes from the neutral lipid used in the study and the phosphate groups on phosphatidylcholine. Other study found that hydrolyzed collagen extracted from Asian sea bass skin affected the ζ -potential of nanoliposomes³⁶. The research findings revealed that liposomes containing PF had a high ζ -potential, suggesting that electrostatic repulsion helps maintain the stability of nanoliposomes and prevents aggregation. Generally, poly-electric charge can adsorb to the surface of liposomes with an opposite charge and modify the ζ -potential.

EE is an important factor in determining nanocarrier stability, showing how well they can keep the inner core from being released^{17,26,37,38}. The EE ranged from 80.90% to 84.10% depending on the type of enzyme used in the study (Table 1). According to Table 1, PFs made with alcalase had the highest EE value at 84% and those made with trypsin had the lowest at 80%. EE was influenced by variations in hydrolysis level and the size of the PFs. In simpler terms, smaller nanoparticles formed by different hydrolysis enzymes are released more quickly from vesicles when the membrane is formed, leading to a decrease in particle size. In a study by Mazloomi et al.³⁹, liposomes and chitosome nano-carriers were created using orange seed PFs and alcalase and pepsin enzymes. They found that PFs made with alcalase had higher EE than those made with pepsin. In this study, all liposomes had EE levels higher than 80%, suggesting they had strong potential for encapsulating PFs.

Antioxidant activity

PFs exhibit antioxidant activity by inhibiting lipid peroxidation, free radicals, and chelating metal ions³². Studying PFs with multiple techniques helps us better understand their antioxidant activity. DPPH and ABTS are stable free radicals with maximum absorption at 517 nm and 734 nm, respectively^{40–42}. When the DPPH and ABTS radicals come into contact with compounds that donate protons, the free radical is blocked and absorption decreases^{7,37}. Figure 1 shows the results of DPPH and ABTS radical scavenging activity evaluation using free peptides and encapsulated peptides. The results showed that both free and encapsulated PF had good antioxidant activity against DPPH and ABTS radicals, ranging from 41 to 81% and 33% to 75%, respectively (Table 2). The study found that there was no significant difference ($p < 0.05$) in the ability to inhibit DPPH and ABTS free radicals between free peptides and encapsulated peptide. The results show that the lipid materials

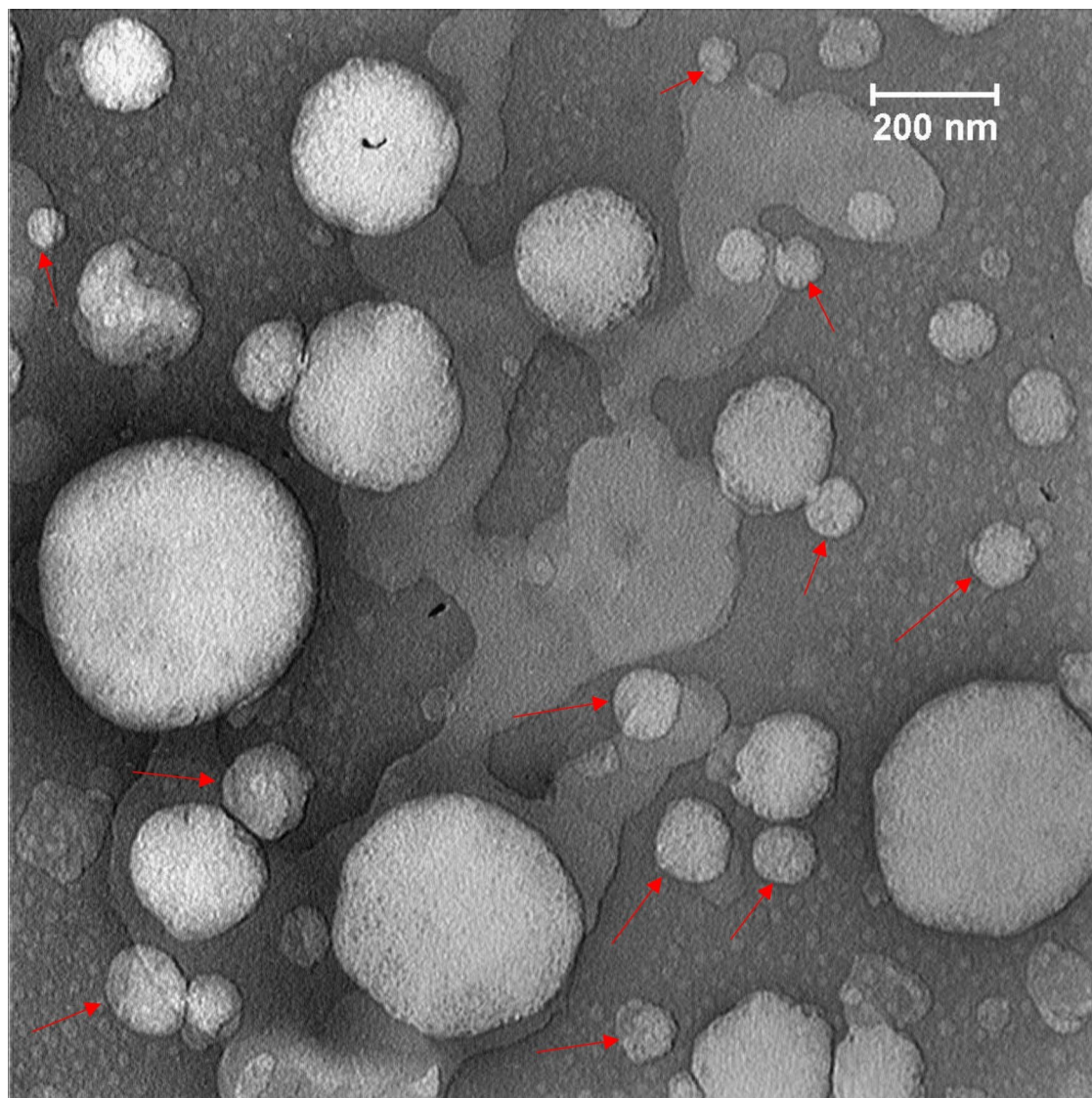


Fig. 1. TEM image of nanoliposome containing peptide.

Enzyme type		DPPH activity (%)	ABTS activity (%)
Cure protein	-	41 ± 1.70 ^d	33 ± 1.60 ^e
Alcalase	Peptide	81 ± 1.50 ^a	72 ± 1.00 ^{ab}
	Encapsulated peptide	79 ± 2.00 ^a	70 ± 0.80 ^b
Pancreatin	Peptide	68 ± 1.90 ^b	75 ± 1.80 ^a
	Encapsulated peptide	65 ± 2.50 ^b	73 ± 2.00 ^a
Trypsin	Peptide	53 ± 1.60 ^c	54 ± 1.10 ^c
	Encapsulated peptide	51 ± 1.90 ^c	47 ± 1.00 ^d

Table 2. The effect of enzyme types on DPPH and ABTS activity of free and nano-encapsulated PFs. Different letters in each column (a, b, c) represents a significant difference between treatments ($p < 0.05$). Data are presented as mean ± SD ($n = 3$).

completely encase the PFs, while still maintaining their biological activity. The study by Hosseini et al.³² found that both free and encapsulated PFs from fish gelatin hydrolysate showed similar antioxidant properties. In contrast, Mosquera et al.⁴³ found out that encapsulating PF from sea bream scales in a partially purified phosphatidylcholine nanocarrier resulted in a two-fold increase in antioxidant activity. It is important to note that encapsulating PFs in liposomes did not affect their antioxidant properties and led to a sustained release

of PFs. Also, these parameters were influenced by the type of hydrolysate enzymes used. Nanoliposomes with alcalase-derived PFs exhibited the strongest DPPH activity (81%), while ABTS activity was highest (75%) in those treated with pancreatin (Table 2). These differences are likely due to enzyme-specific peptide profiles and their hydrophobicity/hydrophilicity, affecting interaction with radicals. The type of amino acid composition is effective in inhibiting DPPH radicals (soluble in fat) and ABTS radicals (soluble in water) due to their different solubility properties.

Based on the results of research on the characteristics and performance of enzymes, since the reaction of PFs and hydrophobic amino acids produced under the influence of alcalase activity with the lipophilic DPPH radical is carried out at a faster rate, therefore these compounds have a higher ability to inhibit this radical compared to they have hydrophilic types (which are released in larger amounts due to the activity of pancreatin enzyme). Research shows that enzymes like alcalase produce PFs and hydrophobic amino acids which react faster with the DPPH radical compared to hydrophilic types released by pancreatin enzyme. This means that these compounds have a higher ability to inhibit the DPPH radical. Daud et al.³¹ and Foh et al.⁴⁴ found similar results when studying how different enzymes affect the rate of inhibition of DPPH and ABTS radical scavenging activity in PFs. Overall, the encapsulation process maintained the antioxidant activity of peptides while improving stability, suggesting their potential use in functional food applications.

Algae hydrolysates made with alcalase were chosen for microencapsulation based on their physicochemical and antioxidant qualities. In the following, the study examined the structure, heat resistance, and morphology of hydrolysates encapsulated by alcalase.

Structural analysis of encapsulated PFs

Morphology of nano-liposomes

Transmission electron microscopy (TEM) images showed that the PF-loaded liposomal vesicles were predominantly spherical to near-spherical with smooth surfaces and clearly defined bilayer boundaries (Fig. 1). Negative-staining TEM commonly used for imaging liposomes provides contrast between the lipid bilayer and the surrounding medium, though drying and staining processes can slightly affect vesicle edge definition^{45,46}. The vesicle population in the micrographs appeared morphologically uniform without evident aggregation or collapse, consistent with homogeneous liposomal systems reported previously⁴⁷.

It is well established that diameters measured by TEM are often smaller than those obtained by dynamic light scattering (DLS), since TEM measures dehydrated or core particle sizes, whereas DLS measures the hydrodynamic diameter in solution^{45,48}. Taken together, the TEM observations support that the PF formulation produced nanoscale lipid vesicles with consistent morphology and intact bilayer structure, corroborating the DLS results and confirming suitability for further physicochemical characterization.

FTIR spectroscopy

FTIR analysis is a powerful method used to determine the structure, accommodation, and phase behavior of components^{16,49}. FTIR analysis confirmed the successful liposomal entrapment of the hydrolysates fraction (Fig. 2). FTIR spectra of free alcalase-hydrolyzed peptides, empty liposomes, and peptide-loaded liposomes (alcalase source) were shown in Fig. 2. The spectrum of free peptide has absorption bands at 3764 cm^{-1} (O–H stretching), 3406 cm^{-1} (N–H stretching), two bands at 2961 and 2930 cm^{-1} (asymmetric C–H stretching of aliphatic chains), 1458 cm^{-1} (bending vibration of CH_2 bonds), 1115 cm^{-1} (C–O stretching vibration), and 621 cm^{-1} (N–H bending) (Fig. 2a). Also, three characteristic bands were observed at 1663 cm^{-1} ; 1549 cm^{-1} ; and 1268 cm^{-1} , originated from short PF chains. These bands correspond to PFs amide I (C=O stretch vibrations and random coils), PFs amide II (C–N stretching and N–H deformation) and PFs amide III (stretching vibration of C–O), respectively (Fig. 2a)^{7,32}.

Empty nanoliposomes show peaks at 3425 cm^{-1} for O–H stretch vibration and, in the range of 2851–2961 cm^{-1} corresponds to symmetric and asymmetric CH_2 stretching vibrations of lipid acyl chains. These peaks indicate properties of the lipid membrane, such as order–disorder state and acyl chain flexibility (Fig. 2b). Hosseini, et al.³² found different signals in the the first part of spectrum due to intense vibrations of OH and NH groups.

Also, some characteristic peaks (Fig. 2b) appeared at 1739 cm^{-1} (C=O stretching vibration of the polar head aliphatic ester groups of phospholipids), 1652 cm^{-1} (C=O stretching vibrations of ester group in phospholipids), 1542 cm^{-1} (N–H bending, amide-II). Additional peaks were observed in the range between 1416 cm^{-1} (CH_2 bending) and 1462 cm^{-1} (C–H bending), peaks at 1245 and 1096 cm^{-1} (asymmetric and symmetric PO_2^- stretching vibrations) and 918 cm^{-1} (asymmetrical stretch vibrations of N^+/CH_3).

After loading the hydrolysates fraction into the liposomal carrier, a great similarity between the IR spectra of hydrolysates fraction and blank phospholipid with the hydrolysates fraction-loaded liposomes was observed (Fig. 2c). The researchers said that the appearance of spectra of both compounds in the structure of liposomal, indicating successful entrapment of the hydrolysate. Although, loading of the hydrolysate into the liposomal carrier changed the FTIR spectra of nanoliposomes, these changes in each of these frequencies indicate the effect of the position of the PF inside the coated nanoliposomes. The FTIR spectra shows the peaks at 1739 and 1652 cm^{-1} (related to blank liposomal) slightly shifted to 1743 and 1654 cm^{-1} respectively, after peptide loading. The slight blue shift from 1739 to 1743 cm^{-1} suggests weakened hydrogen bonding or partial shielding of carbonyl groups due to peptide–lipid interaction. This interaction indicates that the peptides are not merely surface-adsorbed but are likely incorporated within the lipid matrix, which can enhance encapsulation stability and enable sustained release during digestion. Also, the peaks at 3425 cm^{-1} (corresponding to O–H stretching vibrations, in blank nanoliposomes) shifted to a lower frequency (3345 cm^{-1}), accompanied by an increase in peak intensity. These peaks indicate the presence of hydrogen bonds between O–H and N–H groups, which contribute to improved structural integrity and water retention in the hydration shell surrounding the liposomes rather than within the lipid matrix itself³². A minor shift from 2851 to 2854 cm^{-1} , possibly due to the effect of

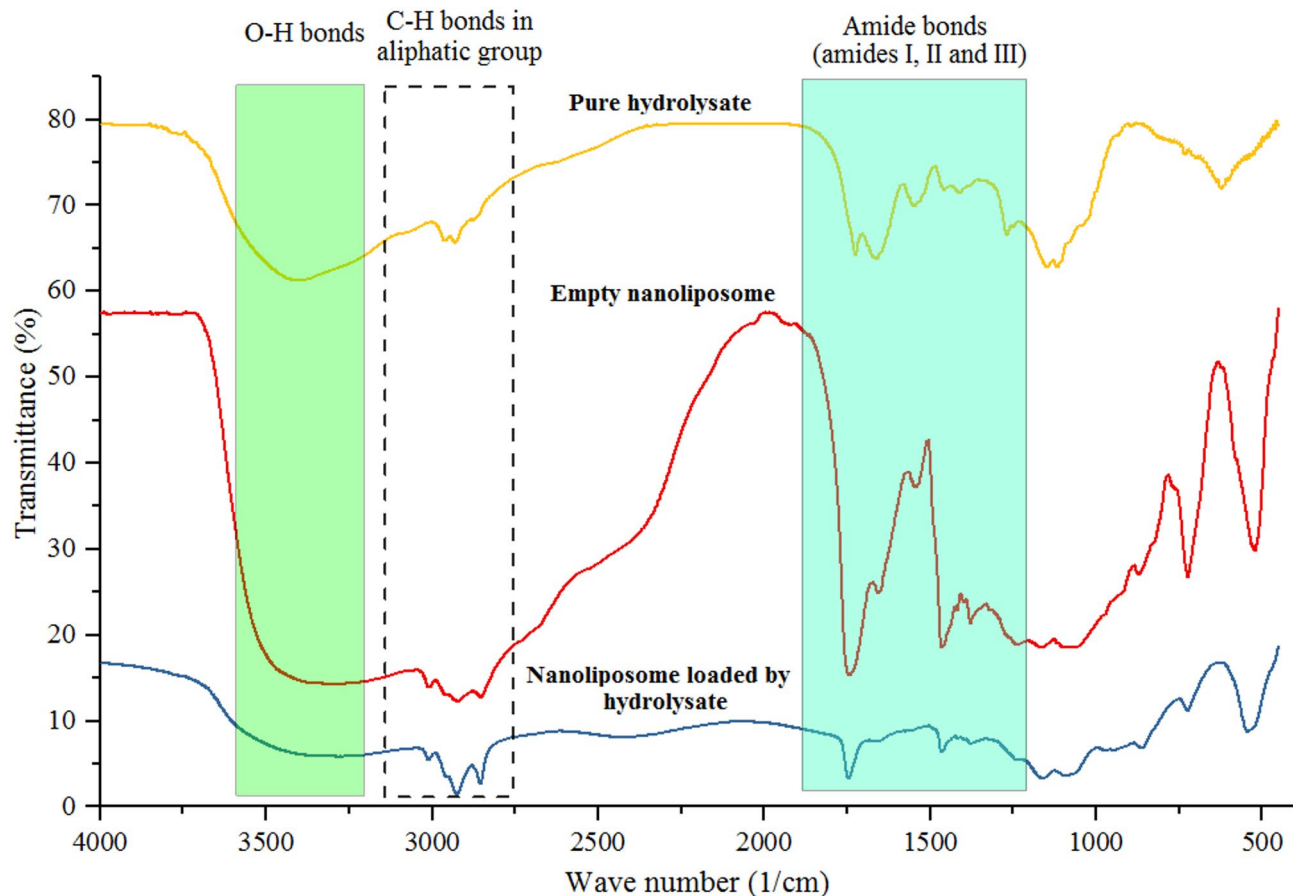


Fig. 2. FT-IR spectra of (a) free peptide, (b), free liposome and (c) encapsulated peptide.

hydrolysates fraction and their placement in the inner region of the nanoliposome monolayer membrane. In the research conducted by Ramezanzade et al.⁵⁰, peaks related to CH_2 stretching vibrations at frequencies of 2921 and 2952 were shifted to higher frequencies in the presence of PFs.

These results align with other researchers' findings regarding the IR spectra of liposome synthesis. Hosseini et al.³² studied the encapsulation of active PF from the fish skin gelatin in the structure of liposomal carrier. These results show that hydrolysate has been successfully encapsulated in the liposomal nanocarrier and is well trapped in the phospholipid bilayer.

DSC analysis

DSC is a thermo-analytical technique that analyze the phase transition in developed liposomal formulations. DSC thermograms were obtained for alcalase-hydrolyzed peptides, blank liposomes, and liposomes encapsulating the same peptides (Fig. 3a–c). The pure PFs exhibited two distinct endothermic transitions at approximately 141 °C and 242 °C, corresponding to the thermal denaturation and subsequent decomposition of the peptide structure. The blank liposomes displayed endothermic events near 110 °C and 203 °C, which are typically associated with the gel-to-liquid crystalline phase transition of the phospholipid bilayer and the rearrangement of lipid chains.

In the case of PF-loaded liposomes, two broader endothermic transitions appeared around 182 °C and 326 °C, markedly different from those observed for both the free peptide and the unloaded lipid vesicles. The presence of these shifted peaks indicates that the peptide was successfully incorporated into the lipid matrix, leading to the formation of strong peptide–lipid interactions (Ramezanzadeh et al. 2021). These interactions likely involve hydrogen bonding and hydrophobic forces between the peptide residues and the polar head groups of lecithin.

The upward shift in transition temperature from 110 °C (blank liposome) to approximately 182 °C (PF-loaded system) reflects a more ordered and rigid bilayer structure, implying that the encapsulated peptides restrict the mobility of the lipid chains. Meanwhile, the broadening and partial merging of the peptide-related peaks (from 141 °C and 242 °C to a wider signal at 182 °C) suggest partial amorphization and dispersion of the peptide within the lipid phase rather than a completely separate crystalline transition.

Overall, the DSC data confirm that PF molecules interact intimately with the lipid bilayer, altering its thermal behavior and enhancing its thermodynamic stability. These findings are consistent with previous observations reported by Caddeo et al.⁵¹ and Ramezanzadeh et al. (2021), who also demonstrated that the incorporation of bioactive peptides into phospholipid matrices modifies bilayer packing and improves the thermal stability of nanoliposomal systems.

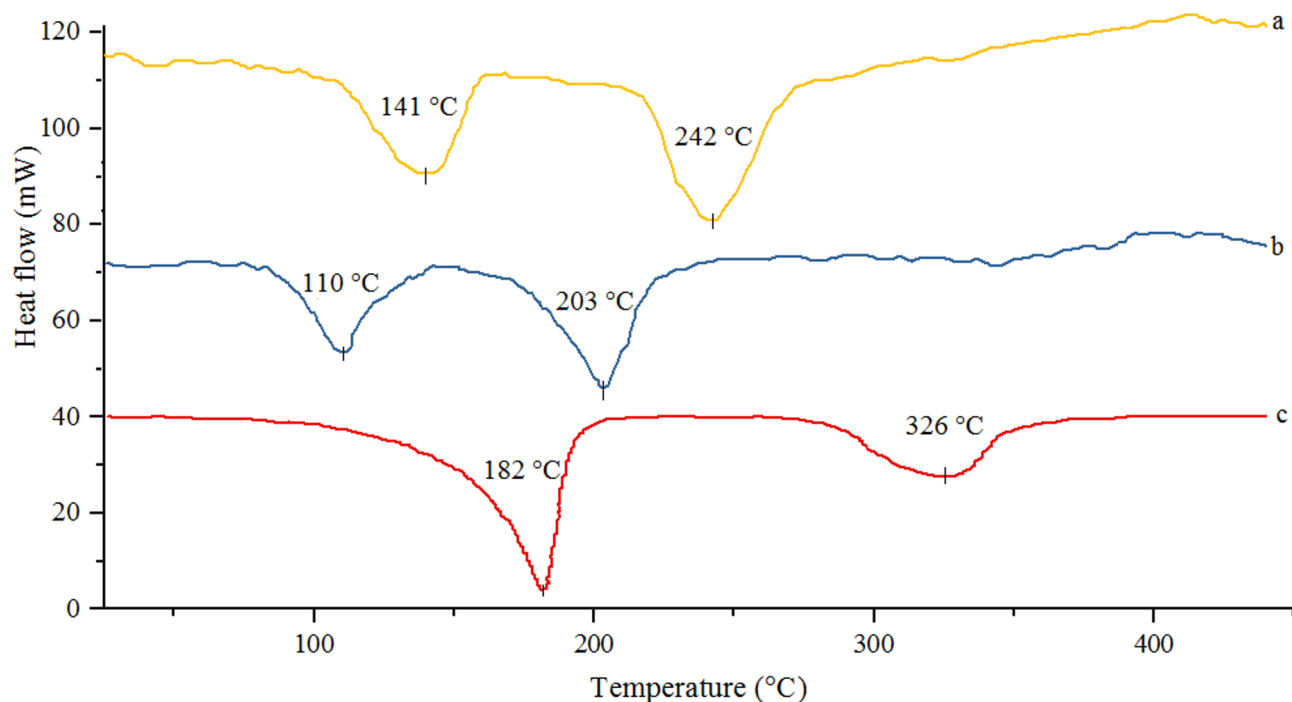


Fig. 3. DSC thermograms of (a) free peptide, (b) blank liposomes and (c) encapsulated peptide.

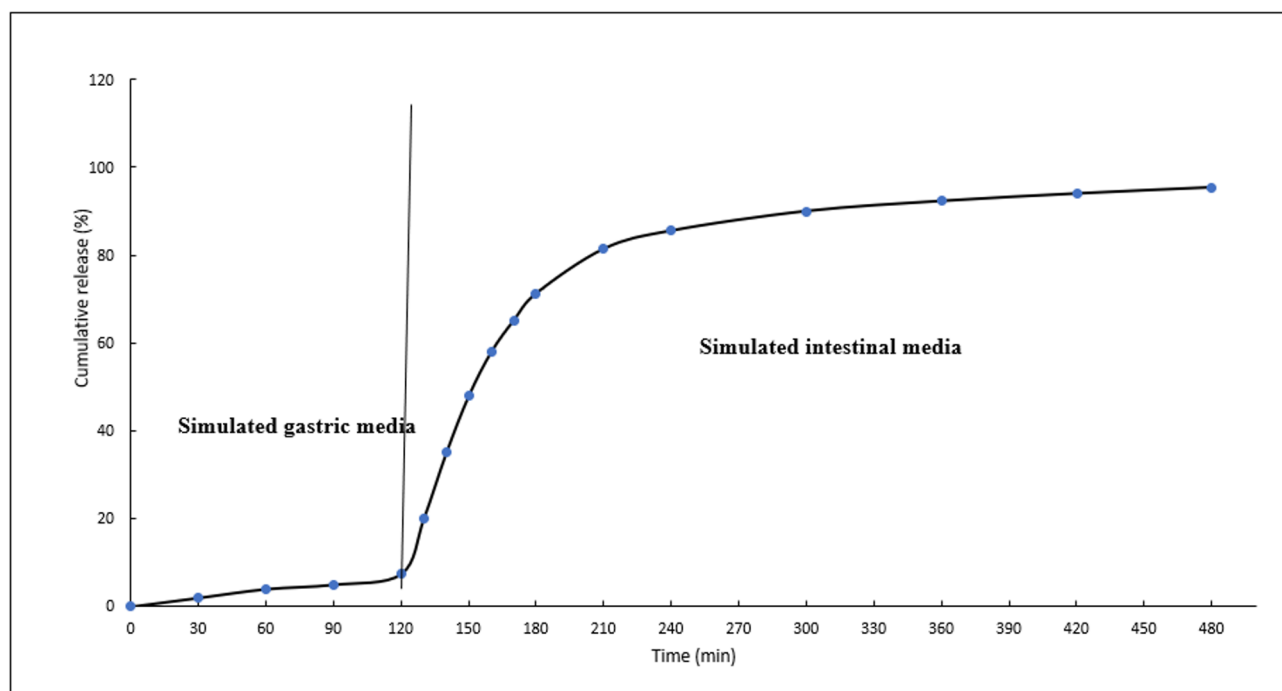


Fig. 4. In-vitro release profiles of the encapsulated peptide in simulated gastric and intestinal media.

In-vitro release test

The key factors in a delivery system are the stability of the active compounds and their timely release from protective structures³⁸. A regular meal takes about 2 h to empty from the stomach²⁹ and 2 to 4 h to pass through the small intestine¹. Therefore, a study was designed to examine the release of PFs in a SGF medium for 2 h and in a SIF medium for 4 h. Figure 4 displays the peptide release in two different media over time intervals. The result shows that the release of the PFs was well controlled and suitable for the conditions in the gastrointestinal tract. During the initial 2 h in SGF medium, approximately 7.45% of the encapsulated peptide was released,

while after 4 h in SIF medium, the release increased to 95.41%. The rapid release in the first hour in the SIF medium is probably due to the surface disposal of PFs adsorbed on the nanoliposome surface. PFs were released slowly after 4 h of digestion due to diffusion through layers of coating, the hydrocarbon part of the membrane, and pores within the membrane. The lowest and the highest percentage of release were seen in the SGF (pH 1.2) and SIF (pH 6.8) media, respectively. In the current study, encapsulated peptide showed limited release in simulated gastric fluid (7.45% over 2 h), indicating strong acid resistance and protection of encapsulated peptides. In contrast, a significant release (95.4%) occurred over 4 h in simulated intestinal fluid, suggesting effective delivery at the target site for absorption¹. At a pH below 6.5, acidic conditions can cause the hydrolysis of saturated phospholipids and lead to instability of liposomes. Also, the instability of encapsulated peptide in SIF medium is caused by the presence of pancreatin, a proteolytic mixture containing lipase, phospholipase, and cholesterol esterase enzymes¹. Therefore, the liposomes destroyed during hydrolysis, allowing the PFs to leak out through pores in the SIF medium. These results are comparable to previous findings. For instance, Ramezanzadeh et al. (2021) reported ~90% peptide release from chitosan-coated liposomes after 4 h in intestinal fluid, while Mohammadi et al.¹⁸ observed only 65–70% release depending on liposome composition. Compared to these studies, the higher release efficiency observed in our formulation indicates enhanced permeability and responsiveness of the liposomal matrix to intestinal enzymes, likely due to optimized particle size and surface charge. Also, the in vitro release pattern observed in our study is consistent with that of Mazloomi et al.³⁹, who reported 12–14% release of orange seed PFs in SGF and up to 91% in SIF using chitosan-coated nanoliposomes. Compared to their system, our formulation demonstrated lower gastric release (7.45%) and higher intestinal release (95.4%), which may be attributed to the smaller vesicle size (68–78 nm) and improved peptide–lipid interactions in our liposomal matrix. These differences suggest enhanced protection under acidic conditions and improved release potential in intestinal environments. The observed release behavior characterized by minimal peptide loss in gastric conditions and nearly complete release in the intestinal phase is considered highly desirable for both functional food and nutraceutical applications. According to previously reported criteria (e.g., (Ramezanzadeh et al. 2021)³⁹, an effective delivery system should ensure <15% release in gastric conditions and >80% release in the intestinal tract to achieve optimal bioavailability and protection. Our system not only meets but exceeds these benchmarks, indicating its potential applicability in real-world formulations where targeted intestinal release is critical.

Conclusion

In this study, bioactive peptide fractions derived from *G. corticata* algae were successfully encapsulated into nanoliposomes using enzymatic hydrolysis and thin-film hydration techniques. Among the enzymes tested, alcalase produced hydrolysates with the highest DH and EE. The resulting peptide-loaded liposomes exhibited favourable physicochemical properties, maintained antioxidant activity, and demonstrated strong resistance to gastric conditions with sustained release in intestinal fluid. Structural and thermal analyses confirmed the successful integration of peptides into the lipid bilayer, enhancing their stability. These findings highlight the potential of nano-liposomal systems as effective carriers for marine-derived peptides in functional foods and nutraceutical products. The delivery profile supports their applicability for targeted intestinal release, which is critical for maximizing release. Future studies should focus on in vivo evaluation, sensory impact in food matrices, and large-scale formulation strategies to validate their industrial feasibility. Despite the promising functional performance of the peptide-loaded nanoliposomal system, this study has certain limitations. Molecular-level characterization of individual peptide sequences was not performed, as the evaluation was primarily focused on functional performance indicators, including degree of hydrolysis, antioxidant activity, physicochemical stability, and gastrointestinal release behavior, which are widely accepted parameters for assessing peptide-based delivery systems. In addition, the encapsulation efficiency determined in this study reflects peptides retained within or strongly associated with the liposomal vesicles, without explicit discrimination between peptides embedded within the lipid bilayer and those weakly adsorbed on the vesicle surface. Future studies may benefit from incorporating advanced analytical techniques, such as mass spectrometry-based peptide profiling and refined separation strategies, to further elucidate peptide composition, structure–activity relationships, and the precise localization of peptides within liposomal carriers.

Data availability

The datasets generated and/or analyzed during the current study are available from the corresponding author on reasonable request.

Received: 23 December 2025; Accepted: 28 March 2026

Published online: 06 May 2026

References

- Molaveisi, M., Shahidi-Noghabi, M. & Naji-Tabasi, S. Controlled release and improved stability of vitamin D3 within nanoliposomes stabilized by palmitic acid. *J. Food Saf.* **41**(5), e12924. <https://doi.org/10.1111/jfs.12924> (2021).
- Salarbashi, D., Tafaghodi, M. & Heydari-Majd, M. Fabrication of curcumin-loaded soluble soy bean polysaccharide/TiO₂ nanoparticles bio-nanocomposite for improved antimicrobial activity. *Nanomed. J.* **7**(10.22038) (2020).
- Tahmouzi, S. et al. Impacts of plant-derived hydrocolloids on technological characteristics of gluten-free bakery products: A comprehensive review. *Compr. Rev. Food Sci. Food Saf.* **25**(1), e70339 (2026).
- Savaghebi, D., Barzegar, M. & Mozafari, M. R. Manufacturing of nanoliposomal extract from *Sargassum boveanum* algae and investigating its release behavior and antioxidant activity. *Food Sci. Nutr.* **8**(1), 299–310. <https://doi.org/10.1002/fsn3.1291> (2020).
- Kumar, D., Agrawal, S., Kumar, M. & Sahoo, D. Assessment of nutritional constituents content and biomedical aspects of five *Gracilaria* species: A multivariate analysis. *J. Aquat. Food Prod. Technol.* **32**(6–7), 570–584 (2023).

6. Rosemary, T., Arulkumar, A., Paramasivam, S., Mondragon-Portocarrero, A. & Miranda, J. M. Biochemical, micronutrient and physicochemical properties of the dried red seaweeds *Gracilaria edulis* and *Gracilaria corticata*. *Molecules* **24**(12), 2225. <https://doi.org/10.3390/molecules24122225> (2019).
7. Mohammadi, M. et al. Engineering of liposome structure to enhance physicochemical properties of *Spirulina plantensis* protein hydrolysate: stability during spray-drying. *Antioxidants* **10** (12), 1953. <https://doi.org/10.3390/antiox10121953> (2021).
8. Quah, Y. et al. Bioactive peptide discovery from edible insects for potential applications in human health and agriculture. *Molecules* **28**(3), 1233. <https://doi.org/10.3390/molecules28031233> (2023).
9. Xie, J., Du, M., Shen, M., Wu, T. & Lin, L. Physico-chemical properties, antioxidant activities and angiotensin-I converting enzyme inhibitory of protein hydrolysates from mung bean (*Vigna radiate*). *Food Chem.* **270**, 243–250. <https://doi.org/10.1016/j.foodchem.2018.07.103> (2019).
10. Farias, T. C. et al. Bioactive properties of peptide fractions from Brazilian soy protein hydrolysates: In silico evaluation and experimental evidence. *Food Hydrocoll. Health* **3**, 100112. <https://doi.org/10.1016/j.fhfh.2023.100112> (2023).
11. Naghdi, S., Lorenzo, J. M., Mirnejad, R., Ahmadvand, M. & Moosazadeh Moghaddam, M. Bioactivity evaluation of peptide fractions from bighead carp (*Hypophthalmichthys nobilis*) using alcalase and hydrolytic enzymes extracted from *Oncorhynchus mykiss* and their potential to develop the edible coats. *Food Bioprocess Technol.* **16**(5), 1128–1148. <https://doi.org/10.1007/s11947-023-02969-0> (2023).
12. Kashyap, R., Narayan, K. S. & Viji, S. Evaluation of the antimicrobial attribute of bioactive peptides derived from colostrum whey fermented by *Lactobacillus* against diarrheagenic *E. coli* strains. *J. Food Sci. Technol.* **60**(1), 211–221. <https://doi.org/10.1007/s13197-022-05504-3> (2023).
13. Félix-Medina, J. V., Sepúlveda-Haro, A. G. & Quintero-Soto, M. F. Stability of antioxidant and hypoglycemic activities of peptide fractions of maize (*Zea mays* L.) under different processes. *J. Food Meas. Charact.* **17**(1), 362–373. <https://doi.org/10.1007/s11694-022-01596-z> (2023).
14. Aldarraj, M. H. et al. *Cyamopsis tetragonoloba* gum-based active coatings incorporated with *Pycnocyba bashgardiana* essential oil for reducing postharvest losses of fresh pistachio fruits. *Food Sci. Nutr.* **13**(7), e70388 (2025).
15. Heydari-Majd, M., Shafeghat, M. & Ghofran-Makshouf, F. Effect of zein nanofiber containing Barije essential oil on increasing the storage time of shrimp (*Litopenaeus vannamei*) at refrigerated temperature (4 ± 1 °C). *Res. Innov. Food Sci. Technol.* **12**(3), 313–328 (2024).
16. Heydari-Majd, M. et al. Electrospun plant protein-based nanofibers loaded with sakacin as a promising bacteriocin source for active packaging against *Listeria monocytogenes* in quail breast. *Int. J. Food Microbiol.* **391**, 110143 (2023).
17. Heydari-Majd, M., Rezaeina, H., Shadan, M. R., Ghorani, B. & Tucker, N. Enrichment of zein nanofiber assemblies for therapeutic delivery of Barije (*Ferula dummosa* Boiss) essential oil. *J. Drug Deliv. Sci. Technol.* **54**, 101290 (2019).
18. Mohammadi, M., Hamishehkar, H., McClements, D. J., Shahvalizadeh, R. & Barri, A. Encapsulation of *Spirulina* protein hydrolysates in liposomes: Impact on antioxidant activity and gastrointestinal behavior. *Food Chem.* **400**, 133973. <https://doi.org/10.1016/j.foodchem.2022.133973> (2023).
19. Karaz, S. & Senses, E. Liposomes under shear: Structure, dynamics, and drug delivery applications. *Adv. Nanobiomed Res.* **3**(4), 2200101. <https://doi.org/10.1002/anbr.202200101> (2023).
20. Ebrahimi, A., Farahpour, M. R., Amjadi, S., Mohammadi, M. & Hamishehkar, H. Nanoliposomal peptides derived from *Spirulina platensis* protein accelerate full-thickness wound healing. *Int. J. Pharm.* **630**, 122457. <https://doi.org/10.1016/j.ijpharm.2023.122457> (2023).
21. Luo, Y. et al. Walnut peptide loaded proliposomes with hydroxyapatite as a carrier: Fabrication, environmental stability, and in vitro digestion attribute. *Food Res. Int.* **162**, 112057. <https://doi.org/10.1016/j.foodres.2022.112057> (2022).
22. Pavlović, N. et al. Ultrasonication for production of nanoliposomes with encapsulated soy protein concentrate hydrolysate: Process optimization, vesicle characteristics and in vitro digestion. *Food Chem. X.* **15**, 100370. <https://doi.org/10.1016/j.fochx.2022.100370> (2022).
23. Ramezanzade, L., Hosseini, S. F., Akbari-Adergani, B. & Yaghmur, A. Cross-linked chitosan-coated liposomes for encapsulation of fish-derived peptide. *LWT* **150**, 112057. <https://doi.org/10.1016/j.lwt.2021.112057> (2021).
24. AOAC. *Official Methods of Analysis* 17th edn. (Association of Official Analytical Chemists, 2005).
25. Bradford, M. M. A rapid and sensitive method for the quantitation of microgram quantities of protein utilizing the principle of protein-dye binding. *Anal. Biochem.* **72**(1–2), 248–254. [https://doi.org/10.1016/0003-2697\(76\)90527-3](https://doi.org/10.1016/0003-2697(76)90527-3) (1976).
26. Bahrami, Z., Pedram-Nia, A., Saeidi-Asl, M., Armin, M. & Heydari-Majd, M. Evaluation of antimicrobial properties of gliadin nanofibers containing *Zataria multiflora* Boiss essential oil and its effect on shelf-life extension of smoked salmon fish fillet. *Res. Innov. Food Sci. Technol.* **11**(2), 141–154 (2022).
27. Majd, M. H., Rajaei, A., Bashi, D. S., Mortazavi, S. A. & Bolourian, S. Optimization of ultrasonic-assisted extraction of phenolic compounds from bovine pennyroyal (*Phlomidioschema parviflorum*) leaves using response surface methodology. *Ind. Crops Prod.* **57**, 195–202. <https://doi.org/10.1016/j.indcrop.2014.03.030> (2014).
28. Abdolshahi, A., Majd, M. H., Abdollahi, M., Fatemizadeh, S. & Marvdashti, L. M. Edible film based on *Lallemantia peltata* L. seed gum: Development and characterization. *J. Chem. Health Risks* **12**(1), 1–13 (2022).
29. Nami, B., Tayebi-Moghaddam, S., Molaveisi, M. & Dehnad, D. Development of soy protein isolate films incorporated with phycoyanin-loaded nanoliposomes to maintain shrimp freshness. *LWT* **196**, 115803. <https://doi.org/10.1016/j.lwt.2024.115803> (2024).
30. Mao, X. Y., Cheng, X., Wang, X. & Wu, S. J. Free-radical-scavenging and anti-inflammatory effect of yak milk casein before and after enzymatic hydrolysis. *Food Chem.* **126**(2), 484–490. <https://doi.org/10.1016/j.foodchem.2010.11.033> (2011).
31. Daud, N. A., Babji, A. S. & Yusop, S. M. Effects of enzymatic hydrolysis on the antioxidative and antihypertensive activities from red tilapia fish protein. *J. Nutr. Food Sci.* **5**(4), 1–5. <https://doi.org/10.4172/2155-9600.1000385> (2015).
32. Hosseini, S. F., Ramezanzade, L. & Nikkhah, M. Nano-liposomal entrapment of bioactive peptidic fraction from fish gelatin hydrolysate. *Int. J. Biol. Macromol.* **105**, 1455–1463. <https://doi.org/10.1016/j.ijbiomac.2017.07.139> (2017).
33. da Rosa Zavareze, E. et al. Production and characterization of encapsulated antioxidative protein hydrolysates from Whitemouth croaker (*Micropogonias furnieri*) muscle and byproduct. *LWT* **59**(2), 841–848. <https://doi.org/10.1016/j.lwt.2014.06.036> (2014).
34. Hoseinpour, Z., Niazmand, R., Parlak, M. E., Heydari-Majd, M. & Saricaoglu, F. T. Shear-thinning dynamics and viscoelasticity of a novel *Eremurus spectabilis* glucomannan: Structural insights and implications for food/pharmaceutical applications. *Carbohydr. Polym. Technol. Appl.* <https://doi.org/10.1016/j.carpta.2025.100910> (2025).
35. Hoseinpour, Z., Niazmand, R. & Heydari-Majd, M. Extraction and characterization of nanocellulose from *Cuminum cyminum* L. husk by ball-milling-assisted ultrasound. *Carbohydr. Polym. Technol. Appl.* <https://doi.org/10.1016/j.carpta.2025.100934> (2025).
36. Chotphruethipong, L., Battino, M. & Benjakul, S. Effect of stabilizing agents on characteristics, antioxidant activities and stability of liposome loaded with hydrolyzed collagen from defatted Asian sea bass skin. *Food Chem.* **328**, 127127. <https://doi.org/10.1016/j.foodchem.2020.127127> (2020).
37. Heydari-Majd, M., Ghanbarzadeh, B., Shahidi-Noghabi, M., Najafi, M. A. & Hosseini, M. A new active nanocomposite film based on PLA/ZnO nanoparticle/essential oils for the preservation of refrigerated *Otolithes ruber* fillets. *Food Packag. Shelf Life* **19**, 94–103 (2019).
38. Heydari-Majd, M. et al. Kinetic release study of zinc from polylactic acid based nanocomposite into food simulants. *Polym. Test.* **76**, 254–260 (2019).

39. Mazloomi, S. N., Mahoonak, A. S., Ghorbani, M. & Houshmand, G. Physicochemical properties of chitosan-coated nanoliposome loaded with orange seed protein hydrolysate. *J. Food Eng.* **280**, 109976. <https://doi.org/10.1016/j.jfoodeng.2020.109976> (2020).
40. Heydari-Majd, M. et al. Poly (lactic acid)-based bionanocomposites: Effects of ZnO nanoparticles and essential oils on physicochemical properties. *Polym. Bull.* **79**(1), 97–119. <https://doi.org/10.1007/s00289-021-03615-4> (2022).
41. Heydari-Majd, M., Monjazeb-Marvdashti, L., Bratovcic, A., Abdolshahi, A., Shadan, M. R. & Yazdani-Dehnavi, M. Prolong the shelf-life and quality attributes of ready-to-eat pomegranate arils using PLA/ZnO nanoparticle/Zataria multiflora essential oil nanocomposite film (2022).
42. Marvdashti, L. M., Arab, S., Bahraminasab, M., Roustaei, M., Souri, S., Majd, M. H. & Abdolshahi, A. Smirnovia Iranica whole herb extract: Antioxidant, radical scavenging, anti-microbial and anti-cancer effects. *J. Chem. Health Risks* **13**(2) (2023).
43. Mosquera, M. et al. Nanoencapsulation of an active peptidic fraction from sea bream scales collagen. *Food Chem.* **156**, 144–150. <https://doi.org/10.1016/j.foodchem.2014.02.011> (2014).
44. Foh, M. B. K., Amadou, I., Foh, B. M., Kamara, M. T. & Xia, W. Functionality and antioxidant properties of tilapia (*Oreochromis niloticus*) as influenced by the degree of hydrolysis. *Int. J. Mol. Sci.* **11**(4), 1851–1869. <https://doi.org/10.3390/ijms11041851> (2010).
45. Baxa, U. Imaging of liposomes by transmission electron microscopy. In *Characterization of Nanoparticles Intended for Drug Delivery* 73–88 (Springer, New York, 2017).
46. Ubhe, A. S. Imaging of liposomes by negative staining transmission Electron microscopy and cryogenic transmission Electron microscopy. In *Liposomes: Methods and Protocols* 245–251 (Springer, New York, 2023).
47. Dymek, M., Olechowska, K., Hąc-Wydro, K. & Sikora, E. Liposomes as carriers of GHK-Cu tripeptide for cosmetic application. *Pharmaceutics* **15**(10), 2485 (2023).
48. Lin, P. C., Lin, S., Wang, P. C. & Sridhar, R. Techniques for physicochemical characterization of nanomaterials. *Biotechnol. Adv.* **32**(4), 711–726. <https://doi.org/10.1016/j.biotechadv.2013.11.006> (2014).
49. Niazmand, R., Sharayei, P., Heydari-Majd, M. & Sayahi, M. Optimization of a novel antimicrobial nanocomposite films based on starch saffron corm incorporating nanoclay/lignin/extract using response surface methodology. *Int. J. Biol. Macromol.* **307**, 141733 (2025).
50. Ramezanzade, L., Hosseini, S. F. & Nikkhal, M. Biopolymer-coated nanoliposomes as carriers of rainbow trout skin-derived antioxidant peptides. *Food Chem.* **234**, 220–229. <https://doi.org/10.1016/j.foodchem.2017.04.177> (2017).
51. Caddeo, C. et al. Cross-linked chitosan/liposome hybrid system for the intestinal delivery of quercetin. *J. Colloid Interface Sci.* **461**, 69–78. <https://doi.org/10.1016/j.jcis.2015.09.010> (2016).

Acknowledgements

This study received a grant from Zahedan University of Medical Sciences, Zahedan, Iran (Project No. 11956; Ethical code: IR.ZAUMS.REC.1404.227).

Author contributions

Mojtaba Heydari-Majd and Farideh Mahmoodi: Investigation, Writing—original draft, Validation, Formal analysis. Hassan Rezaeinia and Ramin Saravani: Writing—review and editing. Mohammad Molaveisi and Mostafa Shahidi Noghabi: Investigation, Writing—original draft, Conceptualization, Methodology, Writing—review and editing, Validation, Supervision, Project administration. Heidar Meftahizade: Writing—review and editing, Supervision. Somayeh Dahmardeh: Writing—review and editing, Writing—review and editing.

Declarations

Competing interests

The authors declare no competing interests.

Additional information

Correspondence and requests for materials should be addressed to R.S. or M.M.

Reprints and permissions information is available at www.nature.com/reprints.

Publisher's note Springer Nature remains neutral with regard to jurisdictional claims in published maps and institutional affiliations.

Open Access This article is licensed under a Creative Commons Attribution-NonCommercial-NoDerivatives 4.0 International License, which permits any non-commercial use, sharing, distribution and reproduction in any medium or format, as long as you give appropriate credit to the original author(s) and the source, provide a link to the Creative Commons licence, and indicate if you modified the licensed material. You do not have permission under this licence to share adapted material derived from this article or parts of it. The images or other third party material in this article are included in the article's Creative Commons licence, unless indicated otherwise in a credit line to the material. If material is not included in the article's Creative Commons licence and your intended use is not permitted by statutory regulation or exceeds the permitted use, you will need to obtain permission directly from the copyright holder. To view a copy of this licence, visit <http://creativecommons.org/licenses/by-nc-nd/4.0/>.

© The Author(s) 2026